Performance of the User in the TDD NOMA Cellular Networks Enabling FFR

Bach-Hung LUU [1], Sinh-Cong LAM [1], Nam-Hoang NGUYEN [1], Trong-Minh HOANG [2]

[1] Faculty of Electronics and Telecommunications, VNU-University of Engineering and Technology, Hanoi, Vietnam
[2] Telecommunication Faculty No1, Posts and Telecommunications Institute of Technology, Hanoi, Vietnam

congls@vnu.edu.vn

Submitted February 3, 2024 / Accepted April 9, 2024 / Online first April 30, 2024

Abstract. *Improving the user performance and spectrum efficiency are urgent problems for 5G and beyond 5G (B5G) cellular networks to support high Quality of Services such as enhanced mobile broadband, ultra-reliable, and low latency communications. Together with Fractional Frequency Reuse (FFR), Time Division Duplex (TDD) and Non-Orthogonal Multi-Access (NOMA) are promising the potential solutions for these problems. While the related researches focus on the single or combination two of three techniques, this paper proposes a system that combination of all three techniques to improve the data rate on the uplink sub-band. Specifically, each couple of Cell-Center User (CCU) and Cell-Edge User (CEU) in a given cell, that is defined by the FFR technique, is allowed to transmit on the same sub-band by the meaning of power-domain NOMA technique. In addition, the TDD technique allow the sharing sub-band between the user and Base Station (BS). The analytical results in Nakagami-m fading and regular path loss model shows that achievable total data rate on the shared sub-band in the proposed system model is 18.2% and 125% higher than that in the regular one with TDD and NOMA, respectively. The data rate improvement of the proposed system model proves the feasibility of co-exits of these techniques in the B5G systems.*

Keywords

Fractional frequency reuse, time division technique, non-orthogonal multiplexing access, Poisson point process

1. Introduction

The high Quality of Service requirements of the users in the recent years have been promoting the development and implementation of the cellular systems such as B5G. In these systems, the radio spectrum is utilized and exploited at a very high efficiency by the advanced techniques to provide a large bandwidth and then a high performance to the users [1]. FFR, which was first introduced for the 4G system and recommended in 3GPP documents, is considered the core technique of the B5G system [1], [2]. In this technique, the BS follows the pre-defined criteria, such as instantaneous received, long-term signal powers and distance from the served users, to classify before serving them on the specific sub-band with appropriate power levels. Through the deployment of FFR technique, the network performance and frequency spectrum can be significantly improved. In addition, TDD and NOMA are emerging as the most potential techniques in the B5G systems [1].

In the previous cellular systems such as 3G and 4G, the uplink and downlink are separated in frequency domain by the meaning of Frequency Division Duplex (FDD) technique. However, due to the asynchronous of uplink and downlink throughput, some of uplink sub-bands are unoccupied while bandwidth shortage can occur in the downlink. Therefore, the TDD technique was introduced to share bandwidth between uplink and downlink [3] so that the spectrum efficiency is improved. The feasibility of the TDD technique on the modern cellular networks has been studied in the literature. In [4], the coverage probability in both uplink and downlink were evaluated in the two-tier system with dynamic and static TDD. The simulation results show that there should be a trade-off between the uplink and downlink performance.The downlink achievable rate of the user in the free-cell system with Multiple-Input-Multiple-Output (MIMO) and TDD technique was studied in [5]. In addition, by proposing a cluster-based radio frame coordination using codebooks, the authors in [6] proved that the uplink performance can be significantly improved while the uplink throughput maintains at a high value. Recently, the combination of TDD with other emerging techniques such as MIMO with and without cooperative communication was studied to enhance the performance of AI-empowered networks [7], [8].

Besides, the NOMA technique was initially developed for 5G networks to allow a BS to simultaneously serve several users on a given sub-band to improve the overall network performance where the users are distinguished by the serving power [9]. The authors in [10] compared the user outage probability in the downlink coordinated multi-point

DOI: 10.13164/re.2024.0312

system with and without NOMA. The paper's results illustrated that there exists a set of network parameters so that the NOMA system achieves a similar outage probability as the system without NOMA. The performance of NOMA technique was studied in the system with energy harvesting [11]. Furthermore, the combination of TDD and NOMA was studied [7, 12, 13]. In [13], the feasibility of TDD - NOMA combination was examined in the system with simultaneous wireless information and power transfer. In addition, the combination of these techniques was also studied in cognitive radio networks [12]. Moreover, the authors in [14] proved that deep reinforcement learning is possible to use to improve the performance of TDD - NOMA system with reconfigurable intelligent surface assistance.

Although the discussed works provided a significant insight about the feasibility NOMA technique in the modern cellular system, he selection of user pair has not been clearly presented. Reference [15] defined the couple of users based on the distance from these users to the serving BSs. Particularly, each user group consists of one near and far users. However, this is not optimal selection since the near users may have better channel qualities than the far ones. Although the channel quality was used in [16] to form the couple of NOMA user, the slow-fading and inter-cell interference were not discussed. In addition, the search on co-exist of TDD and FFR techniques in a cellular system has not been well-investigated. The authosr in [17] discussed the combination of TDD and FFR in the hexagonal cellular network with and without device-to-device links. The study of different FFR schemes in the TDD cellular network with power control was studied in [18]. Although these two works derived the basic knowledge about the operation of cellular networks with both TDD and FFR techniques, the NOMA technique was not presented in these works.

Hence, this paper aims to study the combination of TDD and NOMA techniques in the uplink FFR cellular system. Conventionally, the sub-bands in the regular FFR technique are divided into several orthogonal groups with different operational powers and assigned these sub-band groups to BSs so that the difference between the operational power of a given sub-band in two adjacent BSs is secure. Since this sub-band allocation policy may result in signaling overload between BSs, the modified FFR scheme in this paper allows sharing the same frequency reuse pattern between all BSs. In addition, we form the active users in every cell into CCU - CEU pairs which are distinguished by the uplink SIR. Instead of assuming that the CCU - CEU pairs are served on different sub-bands, the power-domain NOMA technique in this paper allows that this pair of users are served on the same sub-bands but with different serving powers. The Nakagami-m distribution is used to model the fast fading channel due to its general properties. Furthermore, the paper utilizes the stochastic geometry network layout, where the distribution follows the spatial Poisson point process [19], to model the distribution of BSs in the service area. Utilization of PPP model is being widely used to replace the hexagonal cellular network layout since it is close to the practical network deployment [20], [21]. The analytical results from the derived mathematical expressions illustrate that the proposed system can significantly improve the total data rate on the shared sub-band.

The remaining parts of the paper are organized as follows: Section 2 discusses about the PPP network model that simultaneously TDD, modified FFR and NOMA techniques. In addition, the resource allocation schemes and wireless transmission conditions are also presented. Section 3 derives the performance metrics in terms of uplink user coverage probability and data rate. The analytical and simulation results are presented and compared to other related systems in Sec. 4. Finally, the conclusion is drawn in Sec. 5.

2. System Model

In this paper, we study a cellular FFR system that utilizes both TDD and NOMA techniques where the BSs and users are randomly distributed in the service area according to the Spatial Poisson Point Process (PPP) as shown in Fig. 1. Particularly, the number of BSs is a Poisson random variable while their positions follows the spatial PPP. Thus, λ (BS/km^2) called the density of BSs.

The number of active users is large enough so that each BS has at least two users to compose of CCU - CEU pair. Particularly, the user with the lower SIR is defined as CEU and vice versa. In this paper, we assume that the SIR threshold for the definition of CCU and CEU is upon the BS policy. By the meaning of NOMA technique, each pair of CCU and CEU transmit on the same uplink sub-band. Due to the thinning properties of the PPP, CCUs and CEUs are also follows the PPP with the same density of λ_u. In comparison to downlink, the users in uplink tend to transmit a lower volume of data. Thus, there are some unoccupied uplink sub-bands which may be utilized for downlink transmission due to the benefit of TDD technique. Of course, in a given BS, a sub-band only can be used as either downlink sub-band or uplink sub-band. Let λ_b is the density of BSs that utilizes the uplink sub-band to perform data exchange. Then, $\lambda_\mathrm{b} + \lambda_\mathrm{u} = \lambda$.

Figure 1 illustrates an example of an PPP uplink multi-cell proposed network model where the user is at the origin of 2-D coordinate system and within the service area of BS 13. Adjacent BS 2 and BS 14 are used as two different interference sources. Particularly, the BS 2 uses the power-domain NOMA technique to assign the uplink operational band of the typical user for the uplink of CCU and CEU. Thus, the couple of CCU and CEU create interference to the uplink of the typical user which are presented by the dashed red arrows. Since a given sub-band is used in downlink or uplink, the BS 2 does not use the sub-band of CCU and CEU in downlink transmission. Thus, the BS 2 does not create interference to typical user. Meanwhile BS 14 use the uplink operation band of the typical user for downlink transmission. Hence, it directly produces interference to the typical user.

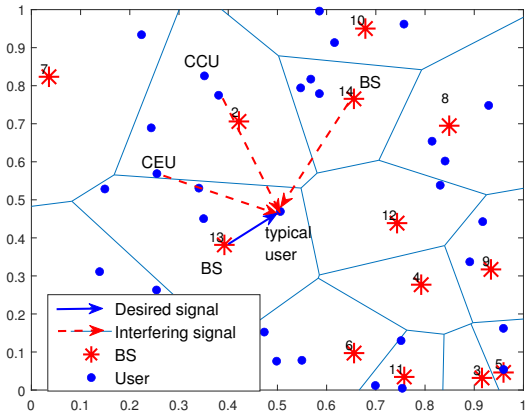

Fig. 1. System layout.

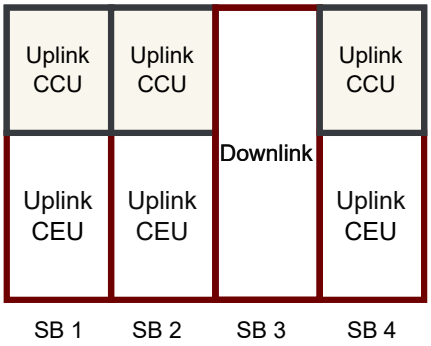

Fig. 2. Uplink and downlink sub-band allocation.

Figure 2 illustrates an example of resource allocation scheme for 4 uplink sub-bands in the proposed system. By the meaning of FFR technique, the uplink signal quality of the users are used to determine CCUs and CEUs. While the traditional FFR technique requires different sub-bands for CCU and CEU, the power-domain NOMA technique is applied to allow the sharing of sub-bands between these users. Particularly, this technique allocates a lower power level for the CCU and a higher one for CEU, which also satisfy the recommendation of FFR technique. In some case, only several allocated uplink sub-bands are used by users for data transmission such as sub-bands SB 1, SB 2, and SB 4. The rest of the uplink sub-bands may be free and wasted. Thanks to the TDD technique, the proposed system can use SB 4 for downlink transmission as illustrated in Fig. 2.

2.1 FFR Technique

With the help of FFR technique, the BSs can simultaneously utilize all sub-bands which are usually partitioned into CC and CE sub-bands with the operational power of P_c and P_e, ($P_e > P_c$), respectively. Conventionally, the user is defined as the CCU and served by power P_c if its downlink SIR on the control channel, SIR, is greater than the classification threshold T, i.e. $SIR > T$ where

$$SIR = \frac{PgL(r)}{\sum_{u\in\theta} Pg_u L(r_u)}. \tag{1}$$

In (1), g and $L(r)$ are the power channel gain and path loss between the user and its serving BS at a distance of r; $\sum_{u\in\theta} Pg_u L(r_u)$ is the total interference from the adjacent BSs in set θ. According to 3GPP document [22], the transmission power of users and BSs in the indoor environment are greater than 20 dBm while the Gaussian noise power is about –103 dBm/Hz. When 20 MHz bandwidth is utilized, the transmission power in each Hz is about –53 dBm/Hz which is extremely greater than the Gaussian noise power. Thus, the impact of Gaussian noise power on the network performance can be omitted. Hence, the Gaussian noise is ignored in the coverage probability and data rate analysis in this paper. In contrast, the CEU should have $SIR < T$. Thus, the CCU and CEU classification probability are defined as the conditional probability $\mathcal{P}_e(T) = \mathbb{P}(SIR < T)$ and $\mathcal{P}_c(T) = 1 - \mathcal{P}_c$. Consequently, the transmission power of the typical user in the FFR system is

$$\begin{cases} P_c & \text{if} \quad SIR > T, \\ P_e & \text{if} \quad SIR < T. \end{cases} \tag{2}$$

The corresponding desired signal power is

$$\begin{cases} P_c g_c L(r) & \text{if} \quad SIR > T, \\ P_e g_e L(r) & \text{if} \quad SIR < T \end{cases} \tag{3}$$

where (g_e, g_c) and $L(r)$ are the power channel gains and path loss between the user and its serving BS at distance r.

2.2 NOMA Technique

While FFR refers to sub-band sharing between BSs, the power-domain NOMA technique allows more than one users use the same sub-band to perform wireless communication with their serving BSs. Conventionally, there is a primary user which can transmit a high transmission power, while others are secondary users and only deploy lower powers. In this paper, we form a CCU and CEU into a pair where the CEU acts as the primary user and CCU is considered the secondary user. Let θ_c and θ_e as the set of CCUs and CEUs. Thus, θ_c and θ_e have the same density of λ_u but each user in θ_c is independent to others in θ_e.

Due to the deployment of FFR and NOMA techniques, the typical user is affected by interference from couples of CCU and CEU at the adjacent cell. Thus, the interfering at the serving BS of the typical user from adjacent cell k is

$$I_k = P_c g L(d_{c,k}) + P_e g_{e,k} L(d_{e,k}) \tag{4}$$

where $d_{c,k}$ and $d_{e,k}$ are the distance from the CCU and CEU at adjacent cell k to the serving BS of the typical user, $g_{c,k}$ and $g_{e,k}$ are the corresponding channel power gains.

Since the set of the adjacent cells of the typical user is θ, the total uplink interference of the typical user is

$$I_u = I_{uc} + I_{ue} \tag{5}$$

where $I_{\text{uc}} = \sum_{k\in\theta_{\text{c}}} P_{\text{c}} g_{\text{c},k} L(d_{\text{c},k})$ and $I_{\text{ue}} = \sum_{k\in\theta_{\text{e}}} P_{\text{e}} g_{\text{e},k} L(d_{\text{e},k})$ are the interference from CCUs and CEUs, respectively.

2.3 TDD Technique

To avoid the waste of unused uplink sub-band, the TDD technique is proposed to used in the system model to allow the BS use some uplink sub-bands as the downlink resource. In this paper, the uplink sub-band is used as a downlink sub-band if and only if it is not used by any user. Let p as the uplink/downlink sharing coefficient to indicate the probability that a uplink sub-band is used by the BS; $p = 0$ if the non of uplink sub-bands are shared to BSs; $p = 1$ if all uplink sub-bands are able to occupied by BSs. Thus, the density of BSs that transmit on the same uplink sub-band is $\lambda_{\text{b}} = p\lambda$. In other words, besides the interfering users at adjacent cells, the BS of the typical user is affected by interference from adjacent BSs with a density of $p\lambda$. The total interference is

$$I_{\text{b}} = \sum_{u\in\theta_{\text{b}}} P_{\text{b}} g_u r_u^{-\alpha}. \tag{6}$$

With assumption that the number of users is large enough so that all uplink sub-bands are utilized, $\lambda_{\text{u}} + \lambda_{\text{b}} = \lambda$. Then, $\lambda_{\text{u}} = (1-p)\lambda$. Consequently, the total interference at the serving BS of the typical user is

$$I = I_{\text{b}} + I_{\text{uc}} + I_{\text{ue}}. \tag{7}$$

Combining with the definition of the desired signal in (3), the uplink SIR of the typical user is

$$SIR = \begin{cases} SIR_{\text{c}} = \frac{P_{\text{c}} g_{\text{c}} L(r)}{I} & \text{if} \quad SIR > T, \\ SIR_{\text{e}} = \frac{P_{\text{e}} g_{\text{e}} L(r)}{I} & \text{if} \quad SIR < T. \end{cases} \tag{8}$$

3. Small-Scale and Large-Scale Fadings

Large-scale fading: In wireless communication, the signal travels over distances usually suffers the path loss due to various conditions such as refraction, reflection, free-space loss and so on. In this paper, the regular path loss model, where the path loss over a distance of r is $L(r) = r^{-\alpha}$, is used to compute the power loss of the signal as it travels from the source to the destination.

Small-scale fading: Since Nakagami-m random variable is able to model the generalized wireless channel, it is adopted in this paper to represent the small-scale fading. Thus, the channel power gain follows normalized gamma random variable with PDF

$$f_{\text{G}}(x) = \frac{m^m x^{m-1}}{\Gamma(m)} \text{e}^{-mx}, \qquad F_{\text{G}}(x) = \frac{\gamma(m, mx)}{\Gamma(m)} \tag{9}$$

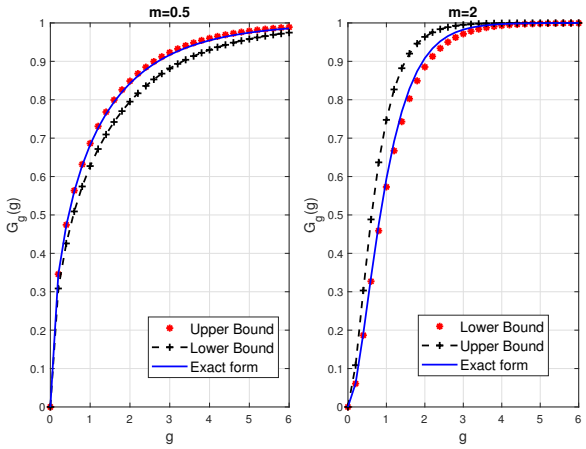

Fig. 3. Upper and lower bound of $F_{\text{G}}(g)$.

where m is the shape of Nakagami random variable; $\gamma(x)$ and $\Gamma(x)$ are the incomplete and complete gamma functions. Utilizing the results in [23], the lower bound and upper bound of $F_{\text{G}}(x)$ is given by

$$m\,(1-\text{e}^{-ax})^m \le F_{\text{G}}(x) \le m\left(1-\text{e}^{-bx}\right)^m \tag{10}$$

where $a = 1$ and $b = \Gamma(m+1)^{-1/m}$ if $m < 1$; and $a = \Gamma(m+1)^{-1/m}$ and $b = 1$ if $m > 1$.

From Fig. 3, it can conclude that $F_{\text{G}}(g) \approx \left(1-\text{e}^{-\zeta x}\right)^m$ where $\zeta = \Gamma(m+1)^{-1/m}$. Utilizing Newton's generalized binomial theorem, $F_{\text{Gr}}(g)$ is expanded as follows:

$$F_{\text{G}}(g) = \sum_{k=0}^{M} \rho(m,k)\text{e}^{-k\zeta x} \tag{11}$$

where $\rho(m,k) = \prod_{h=1}^{k} \frac{m-h+1}{h}$; M is an integer number, and the accuracy of expansion increases with M. In this paper, for sufficient accuracy, $M = m$ if m is an integer number, $M = [m] + 10$ if m is a non-integer number.

4. Performance Evaluation

4.1 Laplace Transform of Intercell Interference

Theorem 4.1 The closed-form expression of Laplace transform of the uplink Interference at the serving BS of the typical user from the CCUs at adjacent cells in the system that utilizes both FFR and NOMA techniques is given by

$$\mathcal{L}_{\text{uc}}(s) = \exp\left[-2\pi\lambda_{\text{u}} C P_{\text{c}}^{\frac{2}{\alpha}} \left(\frac{s}{m}\right)^{\frac{2}{\alpha}}\right], \tag{12}$$

where $C = \left(\sum_{n=1}^{N} C_m^n \frac{(-1)^{n+1}}{2-n\alpha} + \frac{1}{2} + \sum_{n=0}^{N} C_m^n \frac{(-1)^{n+1}}{2+\alpha(m+n)}\right)$.

Proof 4.2 The Laplace transform is defined as $\mathcal{L}_{\text{uc}} = \mathbb{E}\left[\exp\left(-sI_{\text{uc}}\right)\right]$. Substituting the interference's definition in (5), the Laplace transform is expanded by

$$\mathcal{L}_{\text{uc}}(s) = \mathbb{E}\left[\prod_{k\in\theta_{\text{c}}} \exp\left(-sP_{\text{c}}g_{\text{c},k}L(d_{\text{c},k})\right)\right]. \quad (13)$$

Since $g_{\text{c},k}$ and $g_{\text{e},k}$ are a random gamma variable with Laplace transform $E[-sg] = (1+s/m)^{-m}$,

$$\mathcal{L}_{\text{uc}}(s) = \mathbb{E}\left[\prod_{k\in\theta_{\text{c}}} \left(1+\frac{sP_{\text{c}}}{m}L(d_{\text{c},k})\right)^{-m}\right]. \quad (14)$$

Employing the properties of probability generating function with reminding that $0 < d_{\text{c},k} < \infty$ [19],

$$\mathcal{L}_{\text{uc}}(s) = \exp\left[-2\pi\lambda_{\text{u}}\int_0^{\infty}\left(1-\left(1+\frac{sP_{\text{c}}}{mt^{\alpha}}\right)^{-m}\right)t\text{d}t\right]. \quad (15)$$

To compute the integrals in the above equation, we utilize the the binomial expansion formulas of $\frac{1}{(1+x)^m}$ which states that

$$\frac{1}{(1+x)^m} = \begin{cases}\sum_{n=0}^{N} C_m^n(-1)^n x^n & \text{if } x<1,\\ \sum_{n=0}^{N} C_m^n(-1)^n x^{-m-n} & \text{if } x>1\end{cases} \quad (16)$$

where $C_m^n = \binom{n+m-1}{m-1}$; N is an integer number; N is large enough so that the converse of the expansion is obtained. Since $\frac{sP_{\text{c}}}{m}t^{-\alpha} < 1 \Rightarrow t > \left(\frac{sP_{\text{c}}}{m}\right)^{1/\alpha}$, to evaluate the integral $I(P_{\text{c}})$ of (15), we separate it into two parts as follows

$$I_{\text{c}}(P_{\text{c}}) = \int_{(sP_{\text{c}}/m)^{1/\alpha}}^{\infty}\left(1-\left(1+\frac{sP_{\text{c}}}{mt^{\alpha}}\right)^{-m}\right)t\text{d}t + \int_0^{(sP_{\text{c}}/m)^{1/\alpha}}\left(1-\left(1+\frac{sP_{\text{c}}}{mt^{\alpha}}\right)^{-m}\right)t\text{d}t. \quad (17)$$

The first integral in (17) is computed as follows

$$I_{1\text{c}}(P_{\text{c}}) = \int_{\left(\frac{sP_{\text{c}}}{m}\right)^{1/\alpha}}^{\infty}\left(1-\sum_{n=0}^{N}C_m^n(-1)^n\left(\frac{sP_{\text{c}}}{mt^{\alpha}}\right)^n\right)t\text{d}t = \sum_{n=1}^{N}C_m^n(-1)^{n+1}\left(\frac{sP_{\text{c}}}{m}\right)^n\int_{\left(\frac{sP_{\text{c}}}{m}\right)^{1/\alpha}}^{\infty}t^{1-n\alpha}t\text{d}t. \quad (18)$$

Similarity, the second integral in (17) is computed as

$$I_{2\text{c}}(P_{\text{c}}) = \int_0^{\left(\frac{sP_{\text{c}}}{m}\right)^{1/\alpha}}\left(1-\sum_{n=0}^{N}C_m^n(-1)^n\left(\frac{sP_{\text{c}}}{mt^{\alpha}}\right)^{-m-n}\right)t\text{d}t.$$

The integral can be separated into two following parts

$$I_{2\text{c}}(P_{\text{c}}) = \int_0^{\left(\frac{sP_{\text{c}}}{m}\right)^{1/\alpha}} t\text{d}t + \sum_{n=0}^{N}C_m^n(-1)^{n+1}\left(\frac{sP_{\text{c}}}{m}\right)^{-m-n}\int_0^{\left(\frac{sP_{\text{c}}}{m}\right)^{1/\alpha}}t^{1+\alpha(m+n)}\text{d}t.$$

The integrals of $I_{1\text{c}}(P_{\text{c}})$ and $I_{2\text{c}}(P_{\text{c}})$ can directly compute. Hence, $I(P_{\text{c}}) = I_{1\text{c}}(P_{\text{c}}) + I_{2\text{c}}(P_{\text{c}})$ and equals to

$$I(P_{\text{c}}) = \left(\frac{sP_{\text{c}}}{m}\right)^{\frac{2}{\alpha}}\begin{pmatrix}\sum_{n=1}^{N}C_m^n\frac{(-1)^{n+1}}{2-na}+\frac{1}{2}\\ +\sum_{n=0}^{N}C_m^n\frac{(-1)^{n+1}}{2+\alpha(m+n)}\end{pmatrix}.$$

Consequently, the Laplace transform is obtained as in (12). The theorem is proved.

Theorem 4.3 The closed-form expression of Laplace transform of the uplink Interference at the serving BS of the typical user from the CEUs at the adjacent cells in the system that utilizes both FFR and NOMA techniques is given by

$$\mathcal{L}_{\text{ue}}(s) = \exp\left[-2\pi\lambda_{\text{u}}CP_{\text{e}}^{\frac{2}{\alpha}}\left(\frac{s}{m}\right)^{\frac{2}{\alpha}}\right]. \quad (19)$$

Proof 4.4 The only difference between the interference from CCUs and CEUs is the transmission power of the interfering source. Particularly, the transmission power of CCUs is P_{c} while that of CEU is P_{e}. Thus, the Laplace transform of the interference from CEUs can be obtained from Theorem 4.1 by changing the transmission power from P_{c} to P_{e}.

Theorem 4.5 The expression of Laplace transform of the uplink Interference at the serving BS of the typical user from the BSs in the system that utilizes both FFR and NOMA techniques is given by

$$\mathcal{L}_{\text{b}}(s) = \exp\left[-2\pi\lambda_{\text{u}}\int_r^{\infty}\left(1-\left(1+\frac{sP_{\text{b}}}{mt^{\alpha}}\right)^{-m}\right)t\text{d}t\right]. \quad (20)$$

Proof 4.6 Compared to the interfering CCUs, the set of interfering BSs has the following differences. (1) The power of each interfering BS is P_{b}; (2) The density of interfering BSs is λ (3) The interfering BSs should be farther than the serving BS of the typical user, i.e. $r_{\text{u}} > r$. By following the approach in Theorem 4.1, the Laplace transform is obtained.

Theorem 4.7 The Laplace transform of the total interference on a given frequency band is

$$\mathcal{L}(s) = \mathcal{L}_{\text{uc}}(s)\mathcal{L}_{\text{ue}}(s)\mathcal{L}_{\text{b}}(s). \quad (21)$$

Proof 4.8 From (7), the total interference is the sum of I_{ue}, I_{uc}, and I_{b}. Thus, the Laplace transform of the total interference is the product of the corresponding Laplace transform of the interference.

4.2 Coverage Probability

In the cellular system, the coverage probability is used to evaluate the ability to meet signal strength requirements of the typical user. Mathematically, the coverage probability of the typical user with uplink SIR of SIR_{z} defined as:

$$\mathcal{P}_{\mathrm{z}} = \mathbb{P}\left(SIR_{\mathrm{z}} > \hat{T}\right). \tag{22}$$

Thus, the typical user can be either CCU with a probability of $\mathbb{P}(SIR > T)$ and CEU with a probability of $\mathbb{P}(SIR < T)$. Thus, the coverage probability is formulated as:

$$\mathcal{P} = \mathbb{E}_{\mathrm{R}}\left[\mathbb{P}\left(SIR_{\mathrm{c}} > \hat{T}|SIR > T\right) + \mathbb{P}\left(SIR_{\mathrm{e}} > \hat{T}|SIR < T\right)\right].$$

Theorem 4.9 The coverage probability of the CCU in the proposed system is obtained by

$$\mathcal{P}_{\mathrm{c}}(\hat{T}) = \frac{\mathrm{E}\begin{bmatrix}\sum_{k=1}^{M}(-1)^{k+1}\rho(m,k)\mathcal{L}_{\mathrm{b}}(ks_{\mathrm{c}})\mathcal{L}_{\mathrm{uc}}(ks_{\mathrm{c}})\mathcal{L}_{\mathrm{ue}}(ks_{\mathrm{c}})\\ \sum_{h=1}^{M}(-1)^{h+1}\rho(m,h)\mathcal{L}(hs_{\mathrm{b}})\end{bmatrix}}{\mathrm{E}\left[\sum_{h=1}^{M}(-1)^{h+1}\rho(m,h)\mathcal{L}(hs_{\mathrm{b}})\right]}$$

where $s_{\mathrm{c}} = \frac{\zeta\hat{T}r^{\alpha}}{P_{\mathrm{c}}}$; $s_{\mathrm{e}} = \frac{\zeta\hat{T}r^{\alpha}}{P_{\mathrm{e}}}$ and $s_{\mathrm{b}} = \frac{\zeta\hat{T}r^{\alpha}}{P_{\mathrm{b}}}$.

Proof 4.10 Utilizing the definition of SIR in (8), then

$$\begin{aligned}\mathcal{P}_{\mathrm{c}}(\hat{T}) &= \mathbb{P}\left[\frac{P_{\mathrm{c}}g_{\mathrm{c}}L(r)}{I_{\mathrm{b}}+I_{\mathrm{ue}}+I_{\mathrm{uc}}} > \hat{T}\middle|\frac{PgL(r)}{I} > T\right]\\ &= \frac{\mathbb{P}\left[g_{\mathrm{c}} > \hat{T}\frac{I_{\mathrm{b}}+I_{\mathrm{ue}}+I_{\mathrm{uc}}}{P_{\mathrm{c}}L(r)}, g > T\frac{I}{PL(r)}\right]}{\mathbb{P}\left[g > T\frac{I}{PL(r)}\right]}.\end{aligned} \tag{23}$$

From the approximation form of $F_{\mathrm{G}}(g)$ in (11), the coverage probability is approximated by

$$\mathcal{P}_{\mathrm{c}}(\hat{T}) = \frac{\mathrm{E}\begin{bmatrix}\sum_{k=1}^{M}(-1)^{k+1}\rho(m,k)\exp\left(-\frac{\hat{T}k\zeta r^{\alpha}}{P_{\mathrm{c}}}(I_{\mathrm{b}}+I_{\mathrm{ue}}+I_{\mathrm{uc}})\right)\\ \sum_{h=1}^{M}(-1)^{h+1}\rho(m,h)\left[\exp\left(-\frac{Th\zeta r^{\alpha}}{P_{\mathrm{c}}}I\right)\right]\end{bmatrix}}{\mathrm{E}\left[\sum_{h=1}^{M}(-1)^{h+1}\rho(m,h)\left[\exp\left(-\frac{Tk\zeta r^{\alpha}}{P_{\mathrm{c}}}I\right)\right]\right]}.$$

Utilizing the results of Theorems 4.1, 4.3, 4.5, we obtain

$$\mathcal{P}(r) = \frac{\mathrm{E}\begin{bmatrix}\sum_{k=1}^{M}(-1)^{k+1}\rho(m,k)\mathcal{L}_{\mathrm{b}}(ks_{\mathrm{c}})\mathcal{L}_{\mathrm{uc}}(ks_{\mathrm{c}})\mathcal{L}_{\mathrm{ue}}(ks_{\mathrm{c}})\\ \sum_{h=1}^{M}(-1)^{h+1}\rho(m,h)\mathcal{L}(hs_{\mathrm{b}})\end{bmatrix}}{\mathrm{E}\left[\sum_{h=1}^{M}(-1)^{h+1}\rho(m,h)\mathcal{L}(hs_{\mathrm{b}})\right]}$$

where $\mathcal{L}(s_{\mathrm{c}})$ is the Laplace transform of intercell interference on the control channel. Reminding that all users transmit on the control channel at a power of P_{c}, and the density of interfering users on this channel is λ, $\mathcal{L}(s_{\mathrm{c}})$ can be obtained from Theorem 4.1 as follows:

$$\mathcal{L}(s) = \exp\left[-2\pi\lambda C P_{\mathrm{c}}^{\frac{2}{\alpha}}\left(\frac{s}{m}\right)^{\frac{2}{\alpha}}\right]. \tag{24}$$

The theorem is proved.

Theorem 4.11 The coverage probability of the CEU user in the proposed system is given by

$$\begin{aligned}\mathcal{P}_{\mathrm{e}}(\hat{T}) &= \frac{\mathrm{E}\left[\sum_{h=1}^{M}(-1)^{h+1}\rho(m,h)\mathcal{L}(s_{\mathrm{e}})\right]}{1-\mathrm{E}\left[\sum_{h=1}^{M}(-1)^{h+1}\rho(m,h)\mathcal{L}(s_{\mathrm{c}})\right]}\\ &- \frac{\mathrm{E}\begin{bmatrix}\sum_{k=1}^{M}(-1)^{k+1}\rho(m,k)\mathcal{L}_{\mathrm{b}}(ks_{\mathrm{e}})\mathcal{L}_{\mathrm{uc}}(ks_{\mathrm{e}})\mathcal{L}_{\mathrm{ue}}(ks_{\mathrm{e}})\\ \sum_{h=1}^{M}(-1)^{h+1}\rho(m,h)\mathcal{L}(hs_{\mathrm{b}})\end{bmatrix}}{1-\mathrm{E}\left[\sum_{h=1}^{M}(-1)^{h+1}\rho(m,h)\mathcal{L}(hs_{\mathrm{b}})\right]}.\end{aligned}$$

Proof 4.12 Utilizing the definition of SIR in (8),

$$\begin{aligned}\mathcal{P}_{\mathrm{e}}(\hat{T}) =& \mathbb{P}\left[\frac{P_{\mathrm{e}}g_{\mathrm{e}}L(r)}{I_{\mathrm{b}}+I_{\mathrm{ue}}+I_{\mathrm{uc}}} > \hat{T}\middle|\frac{PgL(r)}{I} < T\right]\\ =& \frac{\mathbb{P}\left[g_{\mathrm{e}} > T\frac{I_{\mathrm{b}}+I_{\mathrm{ue}}+I_{\mathrm{uc}}}{P_{\mathrm{e}}L(r)}, g < T\frac{I}{PL(r)}\right]}{\mathbb{P}\left[g > T\frac{I}{PL(r)}\right]}\\ =& \frac{\mathbb{P}\left[g_{\mathrm{e}} > T\frac{I_{\mathrm{b}}+I_{\mathrm{ue}}+I_{\mathrm{uc}}}{P_{\mathrm{e}}L(r)}\right]}{1-\mathbb{P}\left[g > T\frac{I}{PL(r)}\right]} - \frac{\mathbb{P}\left[g_{\mathrm{e}} > T\frac{I_{\mathrm{b}}+I_{\mathrm{ue}}+I_{\mathrm{uc}}}{P_{\mathrm{e}}L(r)}, g > T\frac{I}{PL(r)}\right]}{1-\mathbb{P}\left[g > T\frac{I}{PL(r)}\right]}.\end{aligned}$$

Utilizing the similar approach in Theorem 4.9, the CEU coverage probability is obtained as (25).

4.3 Capacity

This section derives the Shanon capacity of the typical user in the proposed system with TDD and NOMA deployment and the regular TDD one. Theoretically, the capacity of the typical user in the cellular network with received signal quality, SIR_{z}, is allocated an unit bandwidth is defined as

$$C = \mathbb{E}\left[\log_2\left(1+SIR_{\mathrm{z}}\right)\right]. \tag{25}$$

As discussed in the literature, the typical user capacity can be computed by the coverage probability results as follows:

$$\begin{aligned}C &= \int_0^{\infty}\mathbb{P}\left[\log_2\left(1+SIR_{\mathrm{z}}\right) > t\right]\mathrm{d}t\\ &= \int_0^{\infty}\mathbb{P}\left(SIR_{\mathrm{z}} > \mathrm{e}^t-1\right)\mathrm{d}t.\end{aligned} \tag{26}$$

By following the definition of user coverage probability in (22), the typical user capacity is re-written as follows

$$C = \int_0^{\infty}\mathcal{P}_{\mathrm{z}}\left(\mathrm{e}^t-1\right)\mathrm{d}t. \tag{27}$$

In the regular TDD system without NOMA deployment where the users and BSs share the same bandwidth, there are one user and one BS that utilize the same frequency band in each cell. Specifically, the user and BS shares the uplink

sub-band with a probability of p. Thus, the total interference of the shared sub-band in (7) degrades into:

$$\begin{cases} I_{bc} = I_b + I_{uc} & \text{if CCU and BS share sub-band,} \\ I_{be} = I_b + I_{ue} & \text{if CEU and BS share sub-band.} \end{cases} \quad (28)$$

Thus, the total capacity on the sub-band of interest is:

- If the CCU and BS share the same sub-band

$$C_c = \log_2(1 + SIR_{uc}) + p\log_2(1 + SIR_{bc}) \quad (29)$$

  where SIR_{uc} and SIR_{bc} are obtained from (8) by substituting I with I_{bc}.

- If the CEU and BS share the same sub-band

$$C_e = \log_2(1 + SIR_{ue}) + p\log_2(1 + SIR_{be}) \quad (30)$$

  where SIR_{ue} and SIR_{be} are obtained from (8) by substituting I with I_{be}.

In the proposed FFR system with TDD and NOMA combination where each sub-band is shared by the CCU, CEU and BS. Thus, the total capacity on the given sub-band is:

$$C = \log_2(1 + SIR_c) + \log_2(1 + SIR_e) + \log_2(1 + SIR_b)$$

where SIR_c and SIR_e are defined in (8); SIR_b can be obtained from (8) by replacing P_c or P_e with P_b.

5. Simulation and Discussion

In this section, we analyze the coverage probability of the CCU and CEU user with different values of network parameters such as density of BSs, SIR threshold. In addition, the ratio of sharing between the users and BSs is also analyzed.

5.1 Analytical Validation

To validate the analytical results, Monte Carlo simulation technique is utilized in this section. The main procedure of the simulation is described as following steps:

1. Set initial values: λ, p; simulation number N_s; $N_c = 0$; $N_e = 0$.
2. Generate the number of BSs n_b.
3. Generate distance from the typical to all BSs.
4. Generate channel power gains from the typical user to all BSs.
5. Compute SIR on the control channel as in (1) and compare it to the classification threshold T to determine CCU and CEU.
6. With p, the interfering BSs, CCUs, CEUs of the typical user are pn_b, $(1-p)n_b$ and $(1-p)n_b$, respectively.
7. Generate the distance and channel power gains from the typical user to CCUs, CEUs. Noted that the distance to the BSs are generated in Step 2.
8. Compute the SIR_c and SIR_e of CCU and CEU as in (8) and compare with the coverage threshold $\hat{T}$. If $SIR_c > \hat{T}$, $N_c = N_c + 1$. If $SIR_e > \hat{T}$, $N_e = N_e + 1$.
9. Repeat Steps 2–8 N_s times. Thus, the coverage probability of CCU and CEU are N_c/N_s and N_e/N_s.

To make the performance trend closer to the practical network, the analytical and simulation parameters are selected by following the 3GPP recommendation [22]. Specifically, the selected parameters are summarized as Tab. 1.

In Fig. 4, the uplink coverage probability of the CCU, CEU and the typical user are plotted and compared with the Monte Carlo simulation results. As shown in this figure, all theoretical curves visually match with the corresponding simulation ones. This indicates the accuracy of the theoretical analysis in Sec. 4.2.

Since the coverage threshold $\hat{T}$ represents the minimum requirement of SIR power level for the BS to detect the transmitted signal from users. Thus, as shown in Fig. 4, the user coverage probability rapidly reduces with $\hat{T}$ (dB). Specially, when $\hat{T}$ increases from –15 dB to –10 dB, the coverage probability of the typical user declines by around 47% from 0.6 to 0.32. Furthermore, if the typical user can detect the very weak signals which correspond to the very low coverage threshold T, the CCU and CEU coverage probability can reach to the maximum value of 1. In contrast, when the typical user requires very strong signals to perform further processing, its coverage probability can reduce to around 0 or can be called out-of-coverage area.

Parameters	Values
Density of BSs	$\lambda = 1000$ BS/km^2
Path loss coefficient	$\alpha = 3$
CCU transmission power	$P_c = 10$ dBm
CEU transmission power	$P_e = 25$ dBm
BS transmission power	$P_b = 40$ dBm
Nakagami shape	$m = 2$
sub-band sharing probability	$p = 0.4$

Tab. 1. Simulation parameters.

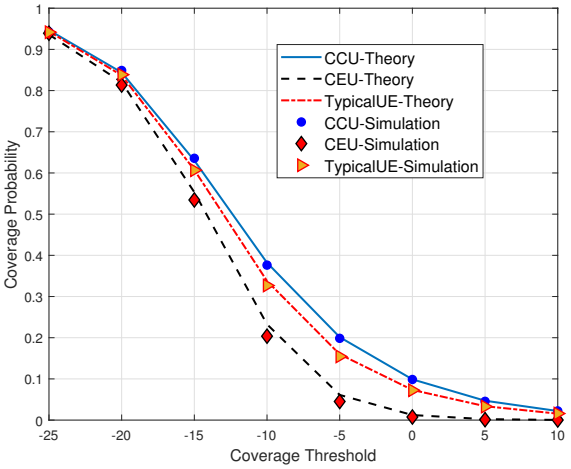

Fig. 4. Theoretical analysis vs simulation.

In the proposed system model, the CCU and CEU have the same statistical properties but the CEU is served by the higher transmission power than the CCU. However, the CCU has a significantly better channel condition than CEU. Thus, the CCU still achieves a higher coverage probability than the CEU as seen in Fig. 4. In addition, the coverage probability of the typical user is the average of CCU and CEU coverage probabilities. Thus, the curve of coverage probability of the typical user lies between that of CCU and CEU.

5.2 Effects of Transmission Power on the User Coverage Probability

In Fig. 5, the impact of BS transmission power on the coverage probability of the typical user is visualized with different values of coverage threshold $\hat{T}$ (dB). Due to the TDD utilization, the BS has a right to utilize the uplink sub-band to perform data transmission and becomes a interference source of the typical user. Consequently, the coverage probability of the typical user reduces. It is obviously that a higher transmission power of BS causes a higher interference power to the typical user and consequently a lower coverage probability. Specially, when the BS transmission power increases from 5 dB to 10 dB, the typical user's coverage probability reduces by 33.3% from 0.6 to 0.4.

5.3 Effects of Sharing Ratio on the User Data Rate

Although deployment of TDD technique results in a decline in the coverage probability of the typical user, this technique can bring benefits to the downlink and overall data rate on the shared sub-band. When the uplink/downlink sharing coefficient p increases, the BS is able to transmit on the uplink with a higher probability. Thus, the downlink data rate on the shared sub-band increases with the coefficient p. As seen from Fig. 6, when p increases by two times from 0.2 to 0.4 and BS transmission power $P_b = 20$ dBm, the data rate increases by 87.8% from 0.33 (bit/s/Hz) to 0.62 (bit/s/Hz).

It is noted that the typical user on the shared sub-band in the proposed system with combination of TDD and NOMA suffers interference from the couple of CCU and CEU in every cell, as well as the adjacent BSs that transmit on this sub-band. Meanwhile, in the system with TDD only, besides interference from adjacent BSs as the same as in the proposed system, the typical user on the shared sub-band is additionally affected by interference from either CCU or CEU. In other words, the typical user in the proposed system suffers a higher interference level than another in the existing one with TDD only. However, the difference between interference levels is relatively small due to the smallness of user transmission power compared to the BS transmission power. Thus, the downlink data rate in the proposed system is very close to the another in the TDD system as shown in Fig. 6.

In addition, when the number of BSs that utilize the uplink sub-band increases with the uplink/downlink sharing coefficient p. Thus, the interference on the shared sub-band increases while the data rate reduces. As the result, the data rate of the couple of CCU and CEU reduces. Upon the changes of p, the total data rate on the shared sub-band reduces or increases. Specifically,

- When p is a small number such as $p < 0.3$ in the case of $P_b = 25$ dBm, the BS operates on the shared sub-band with a very low probability. Thus, the contribution of the downlink data rate on the total data rate of the shared sub-band is very small. Consequently, the total data rate on the shared sub-band reflects the down trend of CCU and CEU data rate. For example, the total data rate reduces by approximately 12% from 1.34 (bit/s/Hz) to 1.18 (bit/s/Hz) as p increases from 0 to 0.3.

- When p is large enough, the BS uses the shared sub-band with a higher density. Thus, the contribution of the downlink data rate on the total data rate of the shared sub-band is remarkable. As the result, the total data rate on the shared sub-band follows the upward of the downlink data rate. Particularly, when p moves from 0.4 to 0.7, the total data rate on the shared sub-band grows by around 6.7% from 1.19 (bit/s/Hz) to 1.27 (bit/s/Hz) in the case $P_b = 25$ dBm.

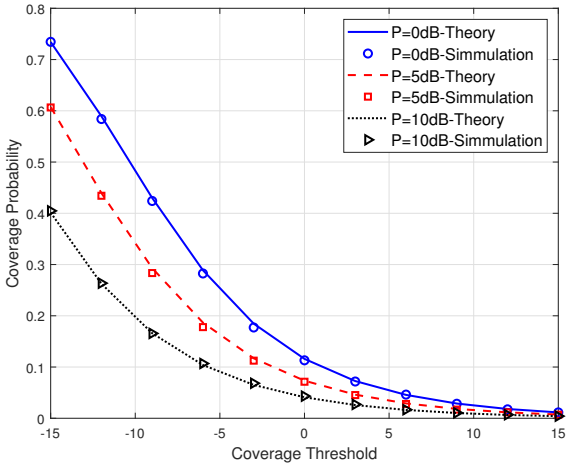

Fig. 5. Coverage probability of typical user vs coverage threshold.

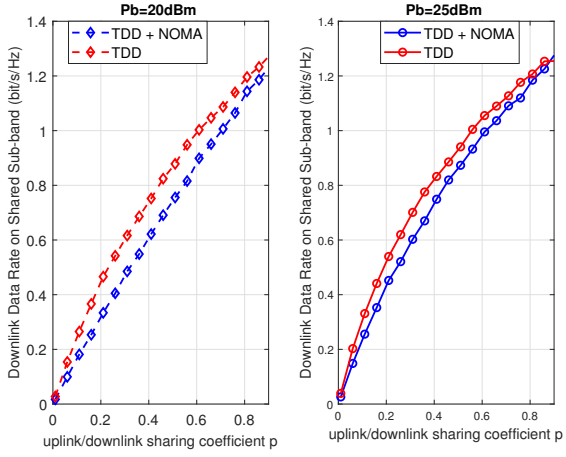

Fig. 6. Downlink data rate on the shared sub-band.

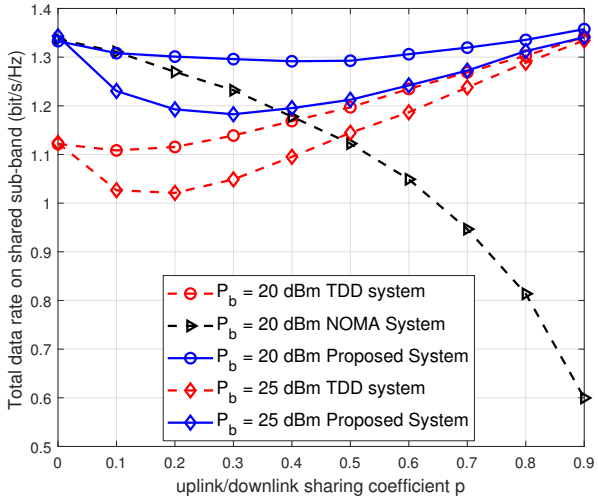

Fig. 7. Data rate on shared sub-band vs sharing coefficient p.

It is also seen from Fig. 7 that the data rate on the shared sub-band in the proposed system is significantly higher than that in the TDD one. Specifically, when the sharing coefficient $p = 0.2$ and $P_b = 20$ dBm which means that the BS is allowed to use 20% of the total uplink sub-bands, the proposed system can provide a data rate of 1.3 (bit/s/Hz) which is 18.2% than that in the TDD system.

In all systems, the users have a higher priority to use the uplink sub-bands and the sharing of uplink sub-band with BSs only takes places if there are some free sub-bands and the TDD technique is enabled. Therefore, the uplink/downlink sharing coefficient in Fig. 7 also indicates the uplink sub-band utilization of the users. For example, $p = 0.3$ means that 70% of uplink sub-bands are utilized by the users, and the rest of sub-band which accounts of 30% can be used by BSs if the TDD technique is enabled. In the system with NOMA technique only, the BSs are unable to the uplink sub-bands through they are free. Thus, the average total data rate on shared sub-band in the NOMA system reduces as p increases. Meanwhile, the proposed system with NOMA and TDD technique, all occupied uplink sub-bands are allocated to the BSs to avoid the waste of sub-band and improve the total data rate on the shared sub-band. Particularly, Figure 7 illustrates that the total data rate on the shared sub-band is at around 1.34 (bit/s/Hz) which is about 125% higher than that in the NOMA system.

6. Conclusion

In this paper, the FFR cellular system that combines TDD and NOMA technique is introduced where each BS selects a couple of CCU and CEU to share the same sub-band. Due to the policy of the FFR and power-domain NOMA techniques, the CCU utilizes a lower power than the CEU to communicate with the serving BS. In addition, the BS is allowed to utilize the uplink sub-band with a predefined probability by the TDD technique. To examine the performance of the typical user in the proposed system, the coverage probability is derived in the wireless condition of Nakagami-m as the fast fading and regular path loss as the slow fading. Through the analytical result, it is stated that the utilization of NOMA technique in uplink TDD system has a very slightly impact on the downlink performance. In addition, the combination of TDD and NOMA techniques in the proposed FFR system can provide a higher total data rate on the shared sub-band of 18.2% and 125% in comparison to the system with TDD and NOMA, respectively. However, there should be more works on the feasibility of TDD, FFR and NOMA techniques. Particularly, the SIR in complicated transmission conditions such as in the indoor area varies by time slot. Thus, the utilization of SIR to classify the CCU and CEU can take place during a very short time and result in a high computing load. In addition, sub-band sharing between users and BSs in the proposed system requires a large amount of signalings which can cause the signaling overload at the BSs.

Acknowledgments

This work has been supported by VNU University of Engineering and Technology under project number CN23.16.

References

[1] AGIWAL, M., ROY, A., SAXENA, N. Next generation 5G wireless networks: A comprehensive survey. *IEEE Communications Surveys & Tutorials*, 2016, vol. 18, no. 3, p. 1617–1655. DOI: 10.1109/COMST.2016.2532458

[2] SONG, M., SHAN, H., YANG, H. H., et al. Joint optimization of fractional frequency reuse and cell clustering for dynamic TDD small cell networks. *IEEE Transactions on Wireless Communications*, 2022, vol. 21, no. 1, p. 398–412. DOI: 10.1109/TWC.2021.3096383

[3] KIM, H., KIM, J., HONG, D. Dynamic TDD systems for 5G and beyond: A survey of cross-link interference mitigation. *IEEE Communications Surveys & Tutorials*, 2020, vol. 22, no. 4, p. 2315–2348. DOI: 10.1109/COMST.2020.3008765

[4] XIE, Z., WU, X., CHEN, X., et al. Coverage analysis of dynamic TDD in two-tier heterogeneous ultra dense networks. In *IEEE 92nd Vehicular Technology Conference (VTC2020-Fall)*. Victoria (BC, Canada), 2020, p. 1–5. DOI: 10.1109/VTC2020-Fall49728.2020.9348431

[5] PAPAZAFEIROPOULOS, A., KOURTESSIS, P., RENZO, M. D., et al. Performance analysis of cell-free massive MIMO systems: A stochastic geometry approach. *IEEE Transactions on Vehicular Technology*, 2020, vol. 69, no. 4, p. 3523–3537. DOI: 10.1109/TVT.2020.2970018

[6] WANG, Y.-C., CHOU, C.-W. Efficient coordination of radio frames to mitigate cross-link interference in 5G D-TDD systems. *Computer Networks*, 2023, vol. 232, p. 1–13. DOI: 10.1016/j.comnet.2023.109840

[7] ZHAO, F., CHEN, W., LIU, Z., et al. Deep reinforcement learning based intelligent reflecting surface optimization for TDD multi-user MIMO systems. *IEEE Wireless Communications Letters*, 2023, vol. 12, no. 11, p. 1951–1955. DOI: 10.1109/LWC.2023.3301496

[8] GE, L. J., NIU, S. X., SHI, C. P., et al. Cascaded deep neural network based adaptive precoding for distributed massive mimo systems. *Radioengineering*, 2024, vol. 33, no. 1, p. 34–44. DOI: 10.13164/re.2024.0034

[9] MAKKI, B., CHITTI, K., BEHRAVAN, A., et al. A survey of NOMA: current status and open research challenges. *IEEE Open Journal of the Communications Society*, 2020, vol. 1, p. 179–189. DOI: 10.1109/OJCOMS.2020.2969899

[10] SUN, Y., DING, Z., DAI, X., et al. Stochastic geometry based modeling and analysis on network NOMA in downlink CoMP systems. *IEEE Transactions on Vehicular Technology*, 2023, vol. 73, no. 1, p. 1–7. DOI: 10.1109/TVT.2023.3301627

[11] TITEL, F., BELATTAR, M. Optimization of NOMA downlink network parameters under harvesting energy strategy using multi-objective GWO. *Radioengineering*, 2023, vol. 32, no. 4, p. 492–501. DOI: 10.13164/re.2023.0492

[12] ALKHAMEES, T. Y., MILSTEIN, L. B. Impact of sharing disruption in MC CR-NOMA. *IEEE Access*, 2023, vol. 11, p. 82871–82881. DOI: 10.1109/ACCESS.2023.3300659

[13] ALAMU, O., OLWAL, T. O., DJOUANI, K. Cooperative NOMA networks with simultaneous wireless information and power transfer: An overview and outlook. *Alexandria Engineering Journal*, 2023, vol. 71, p. 413–438. DOI: 10.1016/j.aej.2023.03.057

[14] KILINC, F., TASCI, R. A., CELIK, A., et al. RIS-assisted grant-free NOMA: User pairing, RIS assignment, and phase shift alignment. *IEEE Transactions on Cognitive Communications and Networking*, 2023, vol. 9, no. 5, p. 1257–1270. DOI: 10.1109/TCCN.2023.3288108

[15] MANKAR, P. D., DHILLON, H. S. Downlink analysis of noma-enabled cellular networks with 3GPP-inspired user ranking. *IEEE Transactions on Wireless Communications*, 2020, vol. 19, no. 6, p. 3796–3811. DOI: 10.1109/TWC.2020.2978481

[16] JAIN, M., SONI, S., SHARMA, N., et al. Performance analysis at far and near user in NOMA based system in presence of SIC error. *AEU - International Journal of Electronics and Communications*, 2020, vol. 114, p. 1–9. DOI: 10.1016/j.aeue.2019.152993

[17] VU, H. V., LE NGOC, T. Performance analysis of underlaid full-duplex D2D cellular networks. *IEEE Access*, 2019, vol. 7, p. 17633–176247. DOI: 10.1109/ACCESS.2019.2958300

[18] FIROUZABADI, A. D., RABIEI, A. M., VEHKAPERA, M. Fractional frequency reuse in random hybrid FD/HD small cell networks with fractional power control. *IEEE Transactions on Wireless Communications*, 2021, vol. 20, no. 10, p. 6691–6705. DOI: 10.1109/TWC.2021.3075987

[19] ANDREWS, J. G., BACCELLI, F., GANTI, R. K. A tractable approach to coverage and rate in cellular networks. *IEEE Transactions on Communications*, 2011, vol. 59, no. 11, p. 3122–3134. DOI: 10.1109/TCOMM.2011.100411.100541

[20] KAVITHA, P., SHANMUGAVEL, S. Analytical evaluation of chunk-based tractable multi-cell OFDMA system. *Radioengineering*, 2018, vol. 7, no. 1, p. 313–325. DOI: 10.13164/re.2018.0313

[21] CHOI, C.-S. Modeling and analysis of downlink communications in a heterogeneous LEO satellite network. *IEEE Transactions on Wireless Communications*, 2024, Early Access, p. 1–15. DOI: 10.1109/TWC.2024.3351876

[22] 3GPP *E-UTRA Further Enhancements to LTE Time Division Duplex (TDD) for Downlink-Uplink (DL-UL) Interference Management and Traffic Adaptation*. 2012, Technical report 3GPP TR 36.828 V11.0.

[23] ALZER, H. On some inequalities for the incomplete gamma function. *Mathematics of Computation*, 1997, vol. 66, no. 218, p. 771–778. DOI: 10.1090/S0025-5718-97-00814-4

About the Authors . . .

Bach-Hung LUU received the Bachelor of Electronic and Communication Engineering Technology from University of Engineering and Technology, Vietnam National University in 2022 and continues his studies towards M.E.

Sinh-Cong LAM (corresponding author) received the Bachelor of Electronics and Telecommunication (Honours) and Master of Electronic Engineering in 2010 and 2012, respectively from University of Engineering and Technology, Vietnam National University (UET, VNUH). He obtained his Ph.D. degree from University of Technology, Sydney, Australia. His research interests focus on modeling, performance analysis and optimization for 5G and B5G, stochastic geometry model for wireless communications

Nam-Hoang NGUYEN received the Ph.D. degree from the Vienna University of Technology, Austria, in 2002. He has been working with the University of Engineering and Technology, Vietnam National University, Hanoi, since 2011, where he was promoted to an Associate Professor in 2018. His research interests include resource management for mobile communications networks and future visible light communications.

Trong-Minh HOANG earned bachelor's degrees in Physics Engineering (1994) and Electronic and Communications Engineering (1999) from Hanoi University of Science and Technology. His master's degree (2003) and Ph.D. degree (2014) in Electronic and Telecommunication Engineering from the Posts and Telecommunications Institute of Technology, Vietnam. He studies wireless network routing, security, and performance in edge computing, sensor networks, wireless mobile networks, and beyond 5G technologies. Assoc. Prof Dr. Trong-Minh Hoang is currently the head of the telecommunication network department and a Senior EEE member.